Published OnlineFirst June 7, 2011; DOI:10.1158/2159-8290.CD-11-0039

CANCER DISCOVERY

High Frequency of *PIK3R1* and *PIK3R2* Mutations in Endometrial Cancer Elucidates a Novel Mechanism for Regulation of PTEN Protein Stability

Lydia W.T. Cheung, Bryan T. Hennessy, Jie Li, et al.

Cancer Discovery 2011;1:170-185. Published OnlineFirst June 7, 2011.

Published OnlineFirst June 7, 2011; DOI:10.1158/2159-8290.CD-11-0039

RESEARCH ARTICLE

High Frequency of *PIK3R1* and *PIK3R2* Mutations in Endometrial Cancer Elucidates a Novel Mechanism for Regulation of PTEN Protein Stability

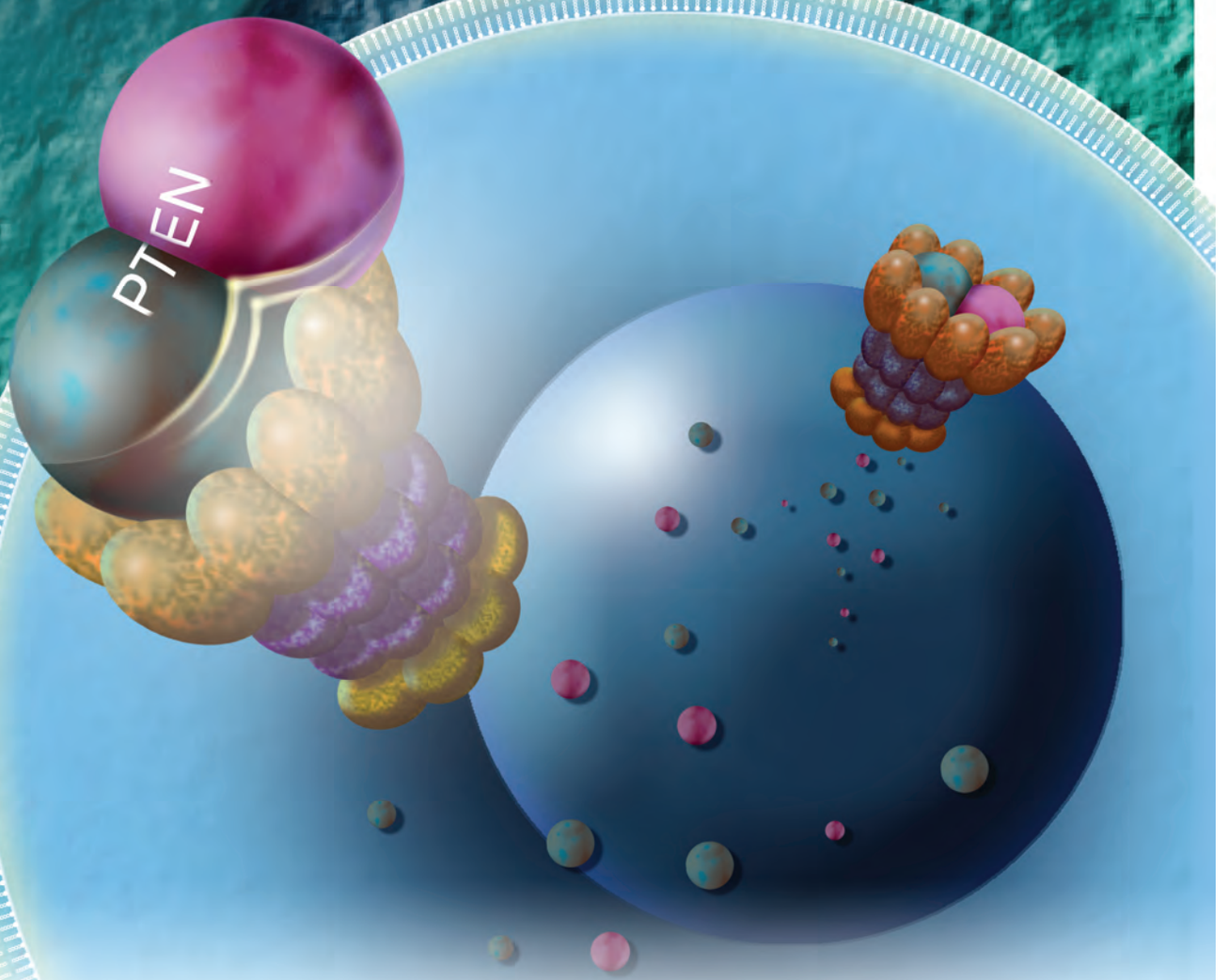

Lydia W.T. Cheung[1,], Bryan T. Hennessy[6,7,*], Jie Li[1], Shuangxing Yu[1], Andrea P. Myers[8,9], Bojana Djordjevic[11], Yiling Lu[1], Katherine Stemke-Hale[1], Mary D. Dyer[1], Fan Zhang[1], Zhenlin Ju[1,2], Lewis C. Cantley[9,10], Steven E. Scherer[5], Han Liang[2], Karen H. Lu[3], Russell R. Broaddus[4], and Gordon B. Mills[1]*

Published OnlineFirst June 7, 2011; DOI:10.1158/2159-8290.CD-11-0039

ABSTRACT

We demonstrate that phosphatidylinositol 3-kinase (PI3K) pathway aberrations occur in >80% of endometrioid endometrial cancers, with coordinate mutations of multiple PI3K pathway members being more common than predicted by chance. *PIK3R1* (p85α) mutations occur at a higher rate in endometrial cancer than in any other tumor lineage, and *PIK3R2* (p85β), not previously demonstrated to be a cancer gene, is also frequently mutated. The dominant activation event in the PI3K pathway appears to be PTEN protein loss. However, in tumors with retained PTEN protein, PI3K pathway mutations phenocopy PTEN loss, resulting in pathway activation. *KRAS* mutations are common in endometrioid tumors activating independent events from PI3K pathway aberrations. Multiple *PIK3R1* and *PIK3R2* mutations demonstrate gain of function, including disruption of a novel mechanism of pathway regulation wherein p85α dimers bind and stabilize PTEN. Taken together, the PI3K pathway represents a critical driver of endometrial cancer pathogenesis and a novel therapeutic target.

SIGNIFICANCE: Our data indicate that the PI3K pathway is targeted in the vast majority of endometrioid endometrial cancers leading to PI3K pathway activation. Frequent oncogenic mutations in *PIK3R1* and *PIK3R2* provide evidence for their role in endometrial cancer pathophysiology with patient-specific mutations revealing a novel mechanism by which p85α regulates the PI3K pathway through stabilizing PTEN. *Cancer Discovery; 1(2);* 170–85. *©2011 AACR.*

INTRODUCTION

Endometrial cancer (EC) is the most prevalent gynecologic malignancy and the fourth most common cancer among women in Western countries. Mortality for localized low-grade, low-stage endometrioid endometrial carcinomas (EEC) is low. However, treatment options for patients with metastatic or recurrent EEC or nonendometrioid endometrial carcinomas (NEEC) are limited and outcomes are extremely poor. Thus there is an urgent need to develop novel effective targeted therapies.

The phosphatidylinositol 3-kinase (PI3K) pathway that signals downstream from receptor tyrosine kinases (RTK) is frequently activated in many cancer lineages, including EC, by aberrations at multiple nodes (1). Inactivation of PTEN, the major negative regulator of the PI3K pathway, has been reported in phenotypically normal endometrium and is sufficient to drive tumorigenesis in mice, suggesting that pathway activation is an early event in EC (2, 3). Loss of PTEN, which can be caused by gene mutation, promoter methylation, and protein degradation, is present in 20% of endometrial hyperplasia, 35% to 50% of EEC, and 10% of NEEC (4–6). Activating *PIK3CA* mutations are present in 30% of EEC and 15% of NEEC and are frequently coexistent with PTEN aberrations (7, 8). Somatic mutations in *AKT1* occur in 2% of EEC (9). Frequent mutations in fibroblast growth factor receptor 2 (*FGFR2)* in EEC (12%) also point to the importance of RTK signaling in the etiology of this disease (10). In addition, other molecular features of EC include gene mutations in pathways that interact with the PI3K pathway, including *CTNNB1* and *TP53* (11, 12).

The PI3K pathway can interact bidirectionally with the Ras/mitogen-activated protein kinase (MAPK) pathway, suggesting that the two pathways might cooperate to determine functional outcomes (13). Activating *KRAS* mutations are found in approximately 20% of EEC (7, 14). However, the significance of the crosstalk between these pathways in EC remains to be explored.

The frequent deregulation of RAS and PI3K signaling in EC offers attractive candidates for targeted therapy. Indeed, compounds that target these pathways are currently in preclinical and clinical development for EC (15, 16). Achievement of optimal therapeutic benefit requires identification of patients likely to benefit combined with rational combinatorial therapy, such as co-targeting of the PI3K and RAS pathways. In this study, we first performed a comprehensive mutational analysis of candidate genes in 243 well-characterized endometrial tumors. Frequent anomalies were found in multiple members of the PI3K

Authors' Affiliations: Departments of [1]Systems Biology, [2]Bioinformatics and Computational Biology, [3]Gynecologic Oncology, and [4]Pathology, The University of Texas MD Anderson Cancer Center; [5]Department of Molecular and Human Genetics, Human Genome Sequencing Center, Baylor College of Medicine, Houston, Texas; [6]Department of Medical Oncology, Beaumont Hospital; [7]Royal College of Surgeons of Ireland, Dublin, Ireland; [8]Division of Women's Cancers, Department of Medical Oncology, Dana-Farber Cancer Institute; [9]Division of Signal Transduction, Department of Medicine, Beth Israel Deaconess Medical Center; [10]Department of Systems Biology, Harvard Medical School, Boston, Massachusetts; and [11]Department of Pathology and Laboratory Medicine, University of Ottawa, Ottawa, Ontario, Canada

*These authors contributed equally to this article.

Note: Supplementary data for this article are available at Cancer Discovery Online (http://www.cancerdiscovery.aacrjournals.org).

Corresponding Author: Lydia W.T. Cheung, Department of Systems Biology, The University of Texas MD Anderson Cancer Center, 7435 Fannin Street, Suite 2SCR3.2211, Houston, TX 77054-1942. Phone: 713-563-0431; Fax: 713-563-4235; E-mail: wcheung@mdanderson.org

doi: 10.1158/2159-8290.CD-11-0039

Published OnlineFirst June 7, 2011; DOI:10.1158/2159-8290.CD-11-0039

pathway and *KRAS*, and the effects of these mutations on downstream signaling were systematically investigated. Second, we determined whether aberrations in the PI3K and MAPK pathways dictate sensitivity toward drugs targeting these pathways. Third, we show for the first time that *PIK3R1* and *PIK3R2*, the genes encoding p85α and p85β, are frequently mutated in EC and novel activating mutations were identified. Finally, we describe a mechanism defined by one of the *PIK3R1* gain of function mutations, which destabilizes PTEN through disruption of p85α homodimerization, offering evidence of the importance of PTEN and p85 interactions in human cancer.

RESULTS

Overview of Nonsynonymous Mutations in EC

In terms of nonsynonymous somatic mutations in 243 endometrial tumors (see Methods), *PTEN* was the most frequently mutated gene (108 tumors, 44%) followed by *PIK3CA* (97 tumors, 40%) (see Fig. 1A and Supplementary Table S1). Moreover, 24 (10%), 39 (16%), and 35 (14%) samples had *FGFR2*, *CTNNB1*, and *TP53* mutations, respectively. *PIK3R1* mutations were detected at a higher frequency (48 tumors, 20%) than in any other cancer lineage (17, 18). Moreover, we found *PIK3R2* mutations, which had not been previously

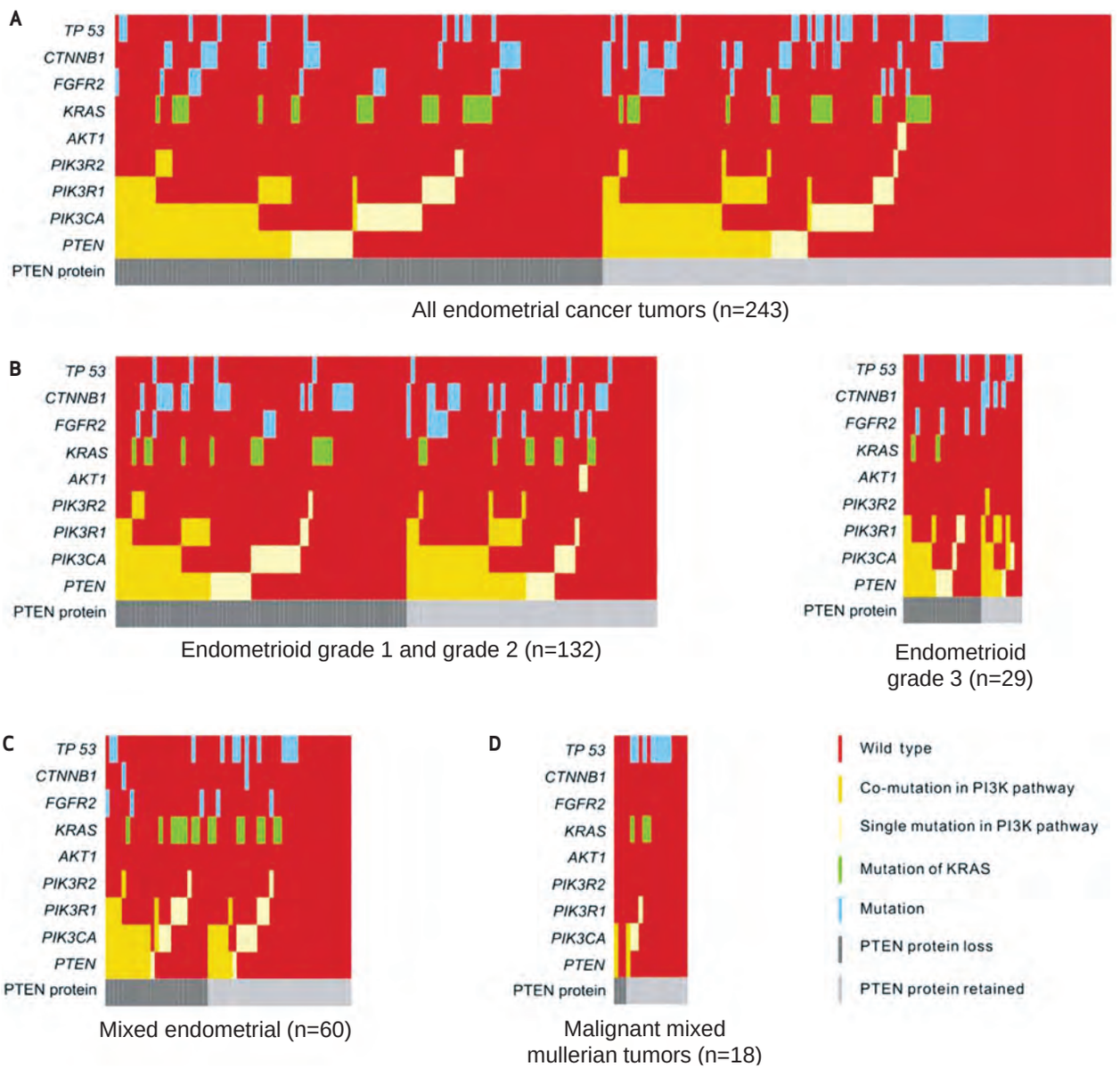

Figure 1. Mutation diagrams: **A**, the full set of endometrial tumor samples ($n = 243$); **B**, endometrioid grade 1 and grade 2 ($n = 132$; left), endometrioid grade 3 ($n = 29$; right); **C**, mixed endometrial ($n = 60$); and **D**, MMMT ($n = 18$). Each column represents a tumor and each row corresponds to a single gene.

Published OnlineFirst June 7, 2011; DOI:10.1158/2159-8290.CD-11-0039

reported at a significant frequency in any tumor lineage, in 12 (5%) endometrial tumors, establishing *PIK3R2* as a cancer-associated gene. A mass spectroscopy–based analysis (MassARRAY, Sequenom) revealed that 43 (18%) and 2 (1%) of the tumors carried mutations in *KRAS* and *AKT1*, respectively, whereas *BRAF, AKT2*, and *AKT3* hotspot mutations were not detected (0%). The majority of the mutations, including those in *PTEN*, were heterozygous.

Expression data from reverse-phase protein array (RPPA) were used to impute PTEN levels where tumor slides for immunohistochemistry (IHC) analysis were unavailable (53 cases) or the staining was heterogeneous (35 cases). Notably, where PTEN expression data were available from both IHC and RPPA, they were concordant in 177 of 190 cases assessed (93%) (Supplementary Fig. S1), suggesting that RPPA allows reliable characterization of PTEN protein levels. Absence of PTEN protein was observed in 119 of 243 (49%) tumors.

The mutation spectrum was similar for tumors defined as EEC and mixed endometrioid and serous carcinomas (Fig. 1B–D and Supplementary Table S1). In contrast, malignant mixed mullerian tumors (MMMT) displayed markedly fewer mutations in the PI3K pathway, no *CTNNB1* mutations, and significantly more frequent *TP53* mutations compared to EEC ($P = 0.001$).

PIK3CA and *PIK3R1* Mutations Frequently Coexist with *PTEN* Heterozygous Mutation

Of particular interest, in contrast to other tumor lineages (19, 20), mutations in *PIK3CA*, *PIK3R1*, *PIK3R2*, *KRAS*, and *PTEN* were not mutually exclusive (Fig. 1). To examine the patterns and frequencies of these co-mutations in detail, we combined data from EEC grades 1, 2, 3, and mixed carcinomas to increase statistical power ($n = 221$, Table 1). *KRAS* mutations frequently coexisted with *PTEN* (7%), *PIK3CA* (8%), or *PIK3R1/PIK3R2* (5%). The co-mutations occurred at frequencies expected based on the frequency of each independent mutation (Supplementary Table S2).

Our data showed that only 10 of 106 (9%) *PTEN* mutations are homozygous with all exhibiting complete loss of PTEN protein (Table 1). Five (50%) of these tumors harbored *PTEN* mutation alone while 5 (50%) had a concomitant PI3K pathway mutation. In contrast, the majority of the heterozygous PTEN-mutant tumors (92%) had coincident mutations in other pathway genes. Strikingly, heterozygous *PTEN* mutation

Table 1. Summary of mutation patterns in the PI3K pathway and *KRAS* in 221 endometrial cancers

	Percentage	PTEN protein		MMR deficient[a]
		Positive	Negative	
All wild type	26.24%	15.38%	10.86%	8/43 (18.60%)
PTEN $^{-/-}$	2.26%	0.00%	2.26%	0/5 (0%)
PTEN $^{+/-}$	6.79%	3.17%	3.62%	2/10 (20%)
PIK3CA	8.60%	3.17%	5.43%	3/16 (18.75%)
PIK3R1/PIK3R2	4.07%	1.36%	2.71%	2/8 (25%)
PIK3CA* + *PIK3R1/PIK3R2	0.90%	0.45%	0.45%	0/2 (0%)
PTEN* $^{-/-}$ + *PIK3CA	1.36%	0.00%	1.36%	1/3 (33.33%)
PTEN* $^{+/-}$ + *PIK3CA	14.93%	9.05%	5.88%	9/30 (30%)
PTEN* $^{-/-}$ + *PIK3R1/PIK3R2	0.45%	0.00%	0.45%	0/1 (0%)
PTEN* $^{+/-}$ + *PIK3R1/PIK3R2	7.24%	4.98%	2.26%	3/15 (20%)
PTEN* $^{-/-}$ + *PIK3CA* + *PIK3R1/PIK3R2	0.45%	0.00%	0.45%	0/1 (0%)
PTEN* $^{+/-}$ + *PIK3CA* + *PIK3R1/PIK3R1	7.69%	3.17%	4.52%	5/17 (29.41%)
KRAS	4.98%	1.81%	3.17%	1/9 (11.11%)
***KRAS* + *PTEN* $^{+/-}$**	1.81%	0.90%	0.90%	2/4 (50%)
KRAS* + *PIK3CA	3.62%	1.81%	1.81%	1/8 (12.5%)
KRAS* + *PIK3R1/PIK3R2	2.71%	0.90%	1.81%	1/5 (20%)
KRAS* + *PTEN* $^{+/-}$ + *PIK3CA	3.17%	1.36%	1.81%	3/6 (50%)
KRAS* + *PTEN* $^{+/-}$ + *PIK3R1/PIK3R2	0.90%	0.45%	0.45%	1/2 (50%)
KRAS* + *PTEN* $^{+/-}$ + *PIK3CA* + *PIK3R1/PIK3R1	0.90%	0.45%	0.45%	1/1 (100%)
AKT	0.90%	0.90%	0.00%	0/2 (0%)

Abbreviations: MMR, mismatch repair; PTEN +/−, PTEN heterozygous mutation; PTEN −/−, PTEN homozygous mutation.

[a] 188 endometrial tumor slides were available and were stained for the MMR proteins.

Published OnlineFirst June 7, 2011; DOI:10.1158/2159-8290.CD-11-0039

frequently co-occurred with *PIK3CA* (59/96; 61%) or *PIK3R1/PIK3R2* (37/96; 39%) mutations (Table 1). The frequencies of these co-mutations were higher than expected due to chance, suggesting mutual inclusivity, in contrast to co-mutations between homozygous *PTEN* and *PIK3CA* or *PIK3R1/PIK3R2* that were present at expected frequencies (Supplementary Table S2). Moreover, 7 of 15 (47%) tumors carrying only heterozygous *PTEN* mutation showed retained PTEN expression, compared to tumors with concomitant mutations in *PIK3CA* (20/33; 61%) or *PIK3R1/PIK3R2* (11/16; 69%). PTEN protein loss was significantly less frequent in tumors with co-mutations in additional pathway members ($P = 0.04$). This observation led us to hypothesize that *PI3KCA*, *PIK3R1*, or *PIK3R2* mutations might be co-selected with heterozygous *PTEN* mutations to compensate for incomplete loss of PTEN protein.

Deficient Mismatch Repair May Contribute to the High Frequency of Co-mutations

Defects in the DNA mismatch repair (MMR) pathway are common in EC, leading to genomic instability (21). Consistent with previous studies, 43 of 188 (23%) tumors were MMR-deficient as indicated by loss on IHC of MLH1, MSH2, or MSH6 (Table 1). Intriguingly, we found MMR deficiency to be significantly more frequent in tumors carrying 2 or 3 PI3K pathway mutations than tumors with 0 or 1 mutation (29% and 32% versus 17% and 19%, respectively; $P < 0.05$). This finding suggested that MMR deficiency might partly contribute to the high frequency of co-mutations in the PI3K pathway in EC. However, the mutations in PI3K pathway members were not classic MMR-related aberrations because they did not occur in regions of nucleotide repeats.

Distribution of *PTEN*, *PIK3CA*, *PIK3R1*, and *PIK3R2* Mutations

Approximately 40% and 60% of PTEN mutations in the endometrial tumor set occur in the C2 and phosphatase domains, respectively (Supplementary Fig. S2). Of 114 *PIK3CA* mutations, 20% were in the adaptor-binding domain (ABD), 17% in the C2 domain, 28% in the helical domain, and 24% were in the kinase domain (Fig. 2A). This distribution is distinct from that observed in other cancers in which the vast majority of mutations cluster within the helical and kinase domains (22, 23). All substitutions in *PIK3R1* were somatic except one known germline single-nucleotide polymorphism (SNP) (M326I). A significant proportion of substitutions (12/29; 41%) and indels (37/42; 88%) were located within the iSH2 domain (Fig. 2B), supporting this region as a mutational hotspot (18). We also detected mutations in all other *PIK3R1* domains, albeit at lower frequencies. Unlike *PIK3R1*, all *PIK3R2* mutations were substitutions with no apparent hotspot region (Fig. 2C). Two alterations observed at the same amino acid, A727T and A727V, were confirmed to be germline SNPs.

PI3K Mutations Functionally Mimic PTEN Loss

The functional impact of PI3K anomalies and the interaction between *KRAS* and PI3K pathway aberration in EC are not well characterized. Therefore, the consequences of these genetic aberrations on downstream signaling were determined by RPPA. Based on the apparent differential effects of PI3K pathway and *KRAS* mutations postulated from the co-mutations, RPPA was assessed in four tumor groups: (1) wild-type (WT) in both PI3K pathway and *KRAS*, (2) PI3K pathway aberrations without *KRAS* mutation, (3) PI3K pathway aberrations with *KRAS* mutation, and (4) *KRAS* mutation only. Levels of phosphorylated AKT (pAKT) at Thr^{308} and Ser^{473}, but not total AKT, were markedly higher in tumors with PI3K pathway aberrations (Supplementary Fig. S3A). *KRAS* mutation was not associated with changes in pAKT. Instead, *KRAS* mutation was associated with increased phosphorylation of mitogen-activated protein kinase kinase (MEK)1/2 at $Ser^{217}/^{221}$, ERK1/2 at Thr^{202}/Tyr^{204}, and p38 MAPK at Thr^{180}/Tyr^{182} without significant change in their respective total proteins (Supplementary Fig. S3B). Activation of the MAPK pathway was not seen in PI3K pathway mutant tumors, suggesting that distinct downstream signaling events are activated in PI3K pathway- and *KRAS*-mutant EC.

PTEN protein loss, regardless of whether PTEN was mutant or WT, was associated with a consistent increase in pAKT indicative of pathway activation (Supplementary Fig. S3C, left). The effect of PTEN loss on pathway activation was dominant because *PIK3CA*, *PIK3R1*, or *PIK3R2* mutation in addition to PTEN loss did not result in a further increase in pAKT (Supplementary Fig. S3C, left). *PTEN* heterozygous mutation alone where PTEN protein was retained was not associated with increased pAKT compared to tumors bearing WT *PTEN* (Supplementary Fig. S3C, right).

Strikingly, in tumors where PTEN protein was retained, including tumors with *PTEN* heterozygous mutation, mutation in other PI3K pathway members, including *PIK3CA*, *PIK3R1*, or *PIK3R2*, resulted in marked increases in pAKT levels comparable to that observed in tumors where PTEN is lost (Fig. 3A and 3B). Furthermore, similar changes in stathmin, caveolin 1, and insulin growth factor binding protein 2 (IGFBP2) were observed in tumors with either PTEN loss or *PIK3CA*, *PIK3R1*, or *PIK3R2* mutations (Fig. 3C). Thus it appears that *PIK3CA*, *PIK3R1*, or *PIK3R2* mutation results in a phenocopy of PTEN loss in terms of pathway activity. These overlapping effects on cellular signaling were also observed in unsupervised hierarchical clustering of the RPPA data, as tumors with PTEN loss intermingled with tumors carrying *PIK3CA*, *PIK3R1*, or *PIK3R2* mutations (Fig. 3A). No significant difference in the pAKT level among tumors carrying *PIK3CA*, *PIK3R1*, or *PIK3R2* mutations or among tumors carrying mutations in different domains of *PIK3CA* or *PIK3R1* (Supplementary Fig. S3D) was detected, suggesting similar effects on cellular function in EC. Together, these data support the functional consequence of *PIK3CA*, *PIK3R1*, or *PIK3R2* mutations on PI3K pathway activation, which is manifest selectively when PTEN is heterozygously mutated and PTEN protein is retained.

Phosphorylation of MEK1/2, ERK1/2, and p38 MAPK was higher in *KRAS*-mutant tumors (Fig. 3D). Strikingly, as with the lack of effect of *KRAS* mutations on PI3K pathway signaling, there was no interaction between the effects of PTEN loss, *PIK3CA*, *PIK3R1*, or *PIK3R2* mutations and the effects of *KRAS* mutation on the MAPK pathway (Fig. 3A).

Together, the signaling data suggest that EC can be robustly classified as either (1) WT PI3K and PTEN-retained,

Published OnlineFirst June 7, 2011; DOI:10.1158/2159-8290.CD-11-0039

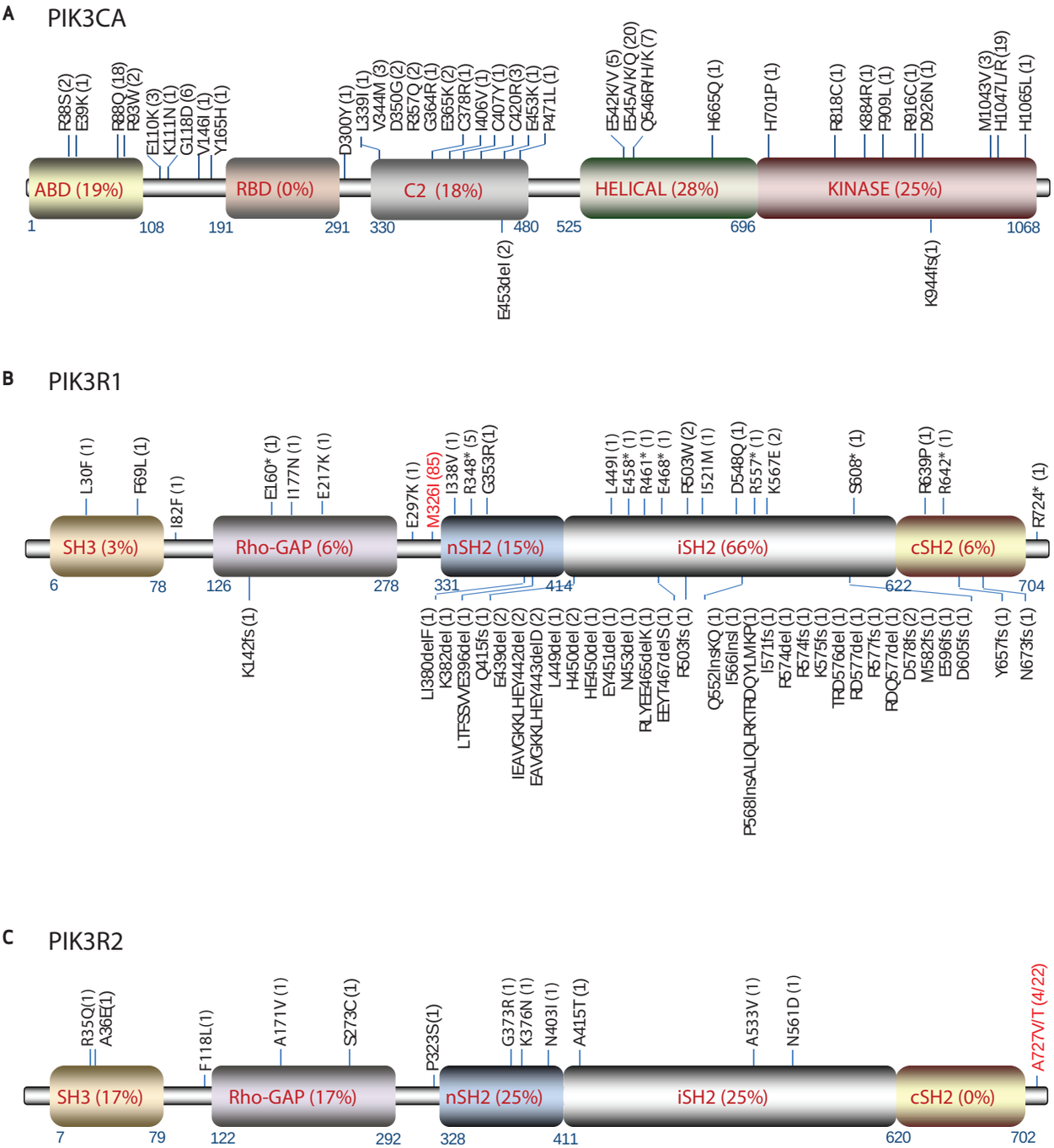

Figure 2. Distribution of nonsynonymous mutations in **A**, *PIK3CA*, **B**, *PIK3R1*, and **C**, *PIK3R2*. Substitutions (top) and indels (bottom) are graphed with the amino acid indicated and the number of independent observations within parentheses. The percentage of mutations identified in each domain is shown in the box. p110α is characterized by 5 domains: ABD, Ras-binding domain (RBD), C2 domain, helical domain, and kinase catalytic domain. p85 consists of SH3, Rho-GAP, and two SH2 domains (nSH2 and cSH2) that flank an intervening domain (iSH2). *, nonsense mutation; bold, mutations confirmed somatic; red, germline SNPs.

or (2) PTEN-lost or PTEN-retained with *PIK3CA*, *PIK3R1*, or *PIK3R2* mutated. The independent effects of *KRAS* mutations in each of the subsets suggest that there are 4 independent groups based on PI3K pathway status and *KRAS* mutation.

Mutation Status Predicts Sensitivity to mTOR and MEK Inhibitors

To determine if mutation status can predict sensitivity to PI3K pathway or MEK inhibitors, we obtained 16 EC cell lines and characterized mutation and signaling status

Published OnlineFirst June 7, 2011; DOI:10.1158/2159-8290.CD-11-0039

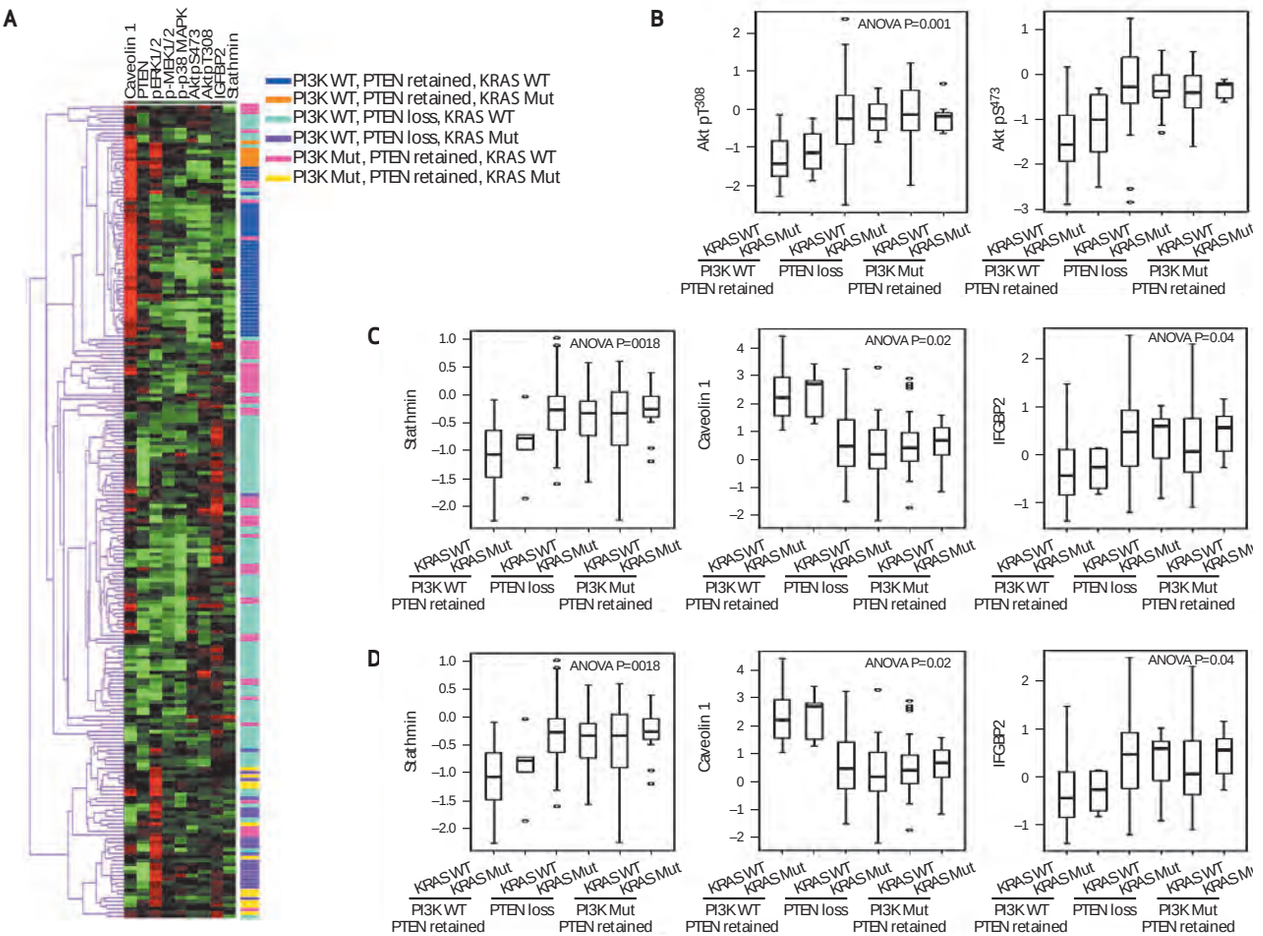

Figure 3. PI3K mutation in tumors where PTEN protein is retained mimics the effect of PTEN loss on downstream signaling regardless of *KRAS* status. **A**, heat map of unsupervised cluster analysis of proteins and samples by RPPA. Proteins are listed across the top of the heat map and mutational status of the tumor is represented at the right. Red, higher expression; green, low relative to the other samples. Expression levels of **B**, phosphorylated AKT at Thr^{308} (left) and Ser^{473} (right); **C**, stathmin (left), caveolin 1 (center), insulin-like growth factor binding protein 2 (IGFBP2; right); **D**, phosphorylated MEK1/2 at $Ser^{217/221}$ (left), ERK1/2 at Thr^{202}/Tyr^{204} (center), and p38 MAPK at Thr^{180}/Tyr^{182} (right) were logarithmically converted, normalized by mean, and presented on the *Y* axis. The boxes represent the distribution of individual values from the lower 25th percentile to upper 75th percentile; solid line in the middle, median value; lower and upper whiskers, 5th and 95th percentiles. WT, wild-type; Mut, mutated.

(Supplementary Table S3). Six of seven (86%) *PTEN* heterozygous mutations co-occurred with *PIK3CA* or *PIK3R1* or *PIK3R2* mutations. As in patient samples, *KRAS* mutation was not mutually exclusive with PI3K pathway mutations.

Loss of PTEN protein was observed in 5 cell lines. More importantly, these 5 cell lines had relatively high pAKT and low caveolin 1 levels as predicted from the patient RPPA data (Supplementary Fig. S4A). Furthermore, Western blot (WB) and RPPA showed that *PIK3CA*, *PIK3R1*, or *PIK3R2* mutations in cells with retained PTEN produced a phenocopy of PTEN loss in terms of activation and expression of the proteins altered in the patient samples (Supplementary Fig. S4).

Cell lines with WT PI3K pathway members were resistant to the mTOR inhibitor rapamycin (Supplementary Fig. S5A). Three cell lines, two of which carry both *KRAS* and *PIK3CA* mutations, were very resistant and a GI_{50} value (concentration needed to achieve 50% growth inhibition) could not be obtained. In contrast, cells with PI3K pathway mutations without *KRAS* mutations were markedly more sensitive to rapamycin. Notably, higher GI_{50} values were obtained in cell lines with concomitant *KRAS* and PI3K pathway mutations than with PI3K pathway mutations alone. There was no obvious correlation between mutational status and responsiveness to GDC-0941, a selective class I PI3K inhibitor that is currently in clinical trials, under the culture conditions assessed (Supplementary Fig. S5B).

All cell lines harboring *KRAS* mutations had concurrent PI3K pathway mutations and were relatively sensitive to MEK inhibition (Supplementary Fig. S5C). However, although cell lines with aberrations in the PI3K pathway tended to be resistant to MEK inhibition, some of the cell lines that lacked *KRAS* mutation were sensitive to MEK inhibition. Thus, *KRAS* mutation is likely a sufficient but not obligatory

Published OnlineFirst June 7, 2011; DOI:10.1158/2159-8290.CD-11-0039

sensitivity marker for MEK inhibitors, which may be useful in patients with *KRAS*-mutant EC.

Identification of Activating Mutations in *PIK3R1* and *PIK3R2*

The majority of *PIK3R1* mutations found in EC are novel and frequent *PIK3R2* mutation has not been reported previously in any tumor lineage. We therefore investigated the functional significance of a subset of these mutations by assessing their ability to induce interleukin-3 (IL-3)–independent survival of Ba/F3 cells, an assay that has been used previously to characterize mutations in PI3K pathway members (18). Three *PIK3R1* indels identified in our dataset (E439del, R574fs, and T576del) were previously characterized and R574fs and T576del have been shown to be oncogenic (24). Concordantly, we found that these two mutants were sufficient to convert Ba/F3 cells to IL-3 independence (Fig. 4A, left). In addition, two truncation mutations—E160* in the Rho-GAP domain that retains the src-homology 3 (SH3) and N terminal proline-rich domain and, with less efficiency, R348* in the nSH2 domain that retains the SH3, Rho-GAP, and two proline-rich domains—and the point mutation R503W in iSH2 conferred IL-3–independent growth to Ba/F3 cells compared with WT p85α or LacZ control. The germline SNP, M326I, had no effect on Ba/F3 survival. It is worth noting that an F268I mutation that was seen in the initial mutation screen but not confirmed in orthologous mutational analysis had no effect on Ba/F3 survival, further confirming the validity of the assay.

We report for the first time herein activating mutations in *PIK3R2* including A171V in the Rho-GAP domain and N561D in the iSH2 domain (Fig. 4A, right). The germline SNP, V727T, had no impact on Ba/F3 survival. WT and E160* *PIK3R1* were assessed in parallel, demonstrating that *PIK3R2* may have greater activity than *PIK3R1* in increasing viability of Ba/F3 cells (Fig. 4A, right, gray bars).

PIK3R1 or *PIK3R2* Activating Mutations Increase AKT Phosphorylation

We sought to understand the mechanism underlying the activity of mutant *PIK3R1* and *PIK3R2* by examining their effects on downstream signaling. The *PIK3R1* or *PIK3R2* mutants that potentiated Ba/F3 cell proliferation increased AKT phosphorylation in the HEC1A EC cell line that contains a G1049R *PIK3CA* and a G12D *KRAS* mutation (Fig. 4B; Supplementary Fig. S6), whereas mutants that had no effect on Ba/F3 survival did not increase pAKT. Indeed, pAKT levels significantly correlated with IL-3-independent survival ($P = 0.001$). There was no observable change in the expression of p110α in cells transfected with any of the mutants. Because p85 binds and stabilizes p110, this suggests that p85α is in excess of p110α in HEC1A cells. Immunoprecipitation (IP) experiments demonstrated that the majority of the mutants retained the ability to bind p110α, except E160* and R348*, which lack the iSH2 domain implicated in p110α binding (Fig. 4C).

The E160* p85α Mutant Destabilizes PTEN

Strikingly, the E160* p85α mutant induced a marked decrease in PTEN protein levels with a concordant increase in pAKT. In contrast, expression of WT p85α led to an increase in PTEN levels, with diminished pAKT in parallel (Fig. 4B, left). The effects of WT p85α on PTEN were confirmed with 3 independent constructs. WT p85β did not alter PTEN or pAKT levels (Fig. 4B, right), suggesting that the two p85 isoforms display different functional consequences in EC. These observations were confirmed with multiple cell lines including EFE184, Ba/F3, and HEK293FT (data not shown).

These changes in PTEN expression are unlikely to have been caused by transcriptional regulation, because PTEN mRNA levels were not altered (data not shown). Rather, cycloheximide-based chase studies demonstrated that WT p85α significantly extended the half-life of PTEN protein (Fig. 5A, left). In contrast, PTEN protein stability in cells transfected with E160* was substantially reduced. Because PTEN protein can be regulated via the ubiquitin-dependent proteasome pathway (25), we treated cells transfected with WT p85α or E160* with the proteasome inhibitor MG132. PTEN protein levels were modestly increased by proteasome inhibition (Fig. 5A, center). Strikingly, E160* enhanced PTEN ubiquitination, whereas WT p85α decreased the abundance of PTEN-ubiquitin conjugates (Fig. 5A, right). These results demonstrated that the ubiquitin degradative pathway likely contributes to the ability of p85α to regulate PTEN protein.

Recent studies have demonstrated the ability of the SH3 and RhoGAP domains of p85α to bind PTEN (26). As indicated in Fig. 5B (left), WT and the other p85α mutants directly interact with PTEN, but not E160*, which lacks the RhoGap domain but retains the BH3 and N terminal proline-rich domain. These observations were confirmed by reciprocal IP (data not shown). Intriguingly, the binding between PTEN and WT p85α was decreased by transfection of increasing amounts of E160* (Fig. 5B, center). The increase in PTEN protein expression and stability induced by WT p85α was also inhibited by co-expression of E160* (Fig. 5B, right). These data suggest that E160* competitively inhibits interactions between PTEN and WT p85α, and this disruption is associated with PTEN destabilization. Additionally, consistent with previous studies (27), we confirmed that WT p85α forms homodimers and this homodimer formation was decreased in the presence of E160* (Fig. 5C, left and center). In parallel, we observed that E160* is able to interact with WT p85α (Fig. 5C, right). These data suggested that homodimerization of WT p85α is inhibited by E160* likely by formation of WT p85α–E160* dimers. This process is associated with diminished binding between WT p85α and PTEN. Furthermore, overexpression of p110α disrupted the interaction between WT p85α and E160*, formation of WT p85α homodimer and binding of PTEN to p85α (Fig. 5D), suggesting that binding of p110α and PTEN to p85α is mutually exclusive and that p110α does not bind to the PTEN–p85α homodimer complex.

DISCUSSION

Characterization of mutations in cancer cells provides insights into tumorigenesis and reveals candidates for targeted therapeutics. Most previous studies of genetic aberrations in EC are small with analysis of a limited number of candidate genes. The functional relevance of these alterations in EC is

Published OnlineFirst June 7, 2011; DOI:10.1158/2159-8290.CD-11-0039

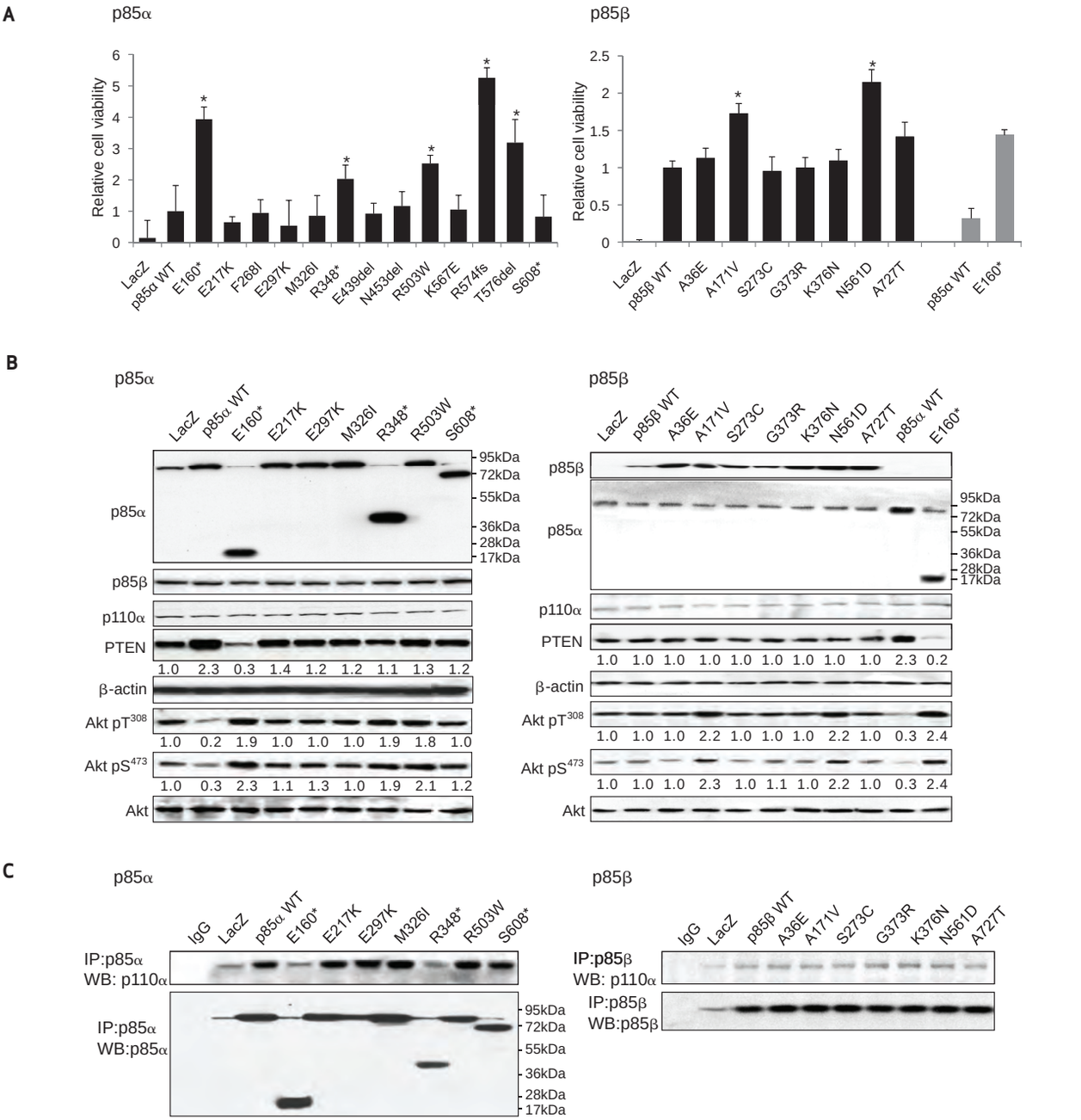

Figure 4. Ba/F3 cells were transfected with **A**, WT p85α (p85α WT, left) or patient mutants, or WT p85β or patient mutants (right two gray bars, p85α WT or E160*). Cells were cultured without IL-3 for 4 weeks and harvested for viability assay. LacZ served as the control. The means (±SD) of triplicate samples of 3 independent experiments are shown. *, $P < 0.05$, compared with WT. The plasmids were transiently transfected into HEC1A cells. Whole-cell lysates were collected at 72 hours post-transfection for **B**, WB or **C**, IP with anti-p85α and then subjected to WB with anti-p110α. Numerical values below each lane of the immunoblots represent quantification of the relative protein level by densitometry (normalized to β-actin or AKT).

also obscure, hampering the development and implementation of pathway-targeted therapy. Therefore, we performed an integrated analysis to determine the effects of a broad set of candidate mutations on downstream signaling in a large sample set. In agreement with the model of type 1 EC (endometrioid/mucinous) (7, 11, 12), the EEC in our dataset are characterized by high frequencies of aberrations in the PI3K pathway, *KRAS*, and *CTNNB1*, whereas *TP53* mutations are more frequent in grade 3 EEC. The mixed endometrioid/serous histotype is genetically similar to EEC, suggesting that

Published OnlineFirst June 7, 2011; DOI:10.1158/2159-8290.CD-11-0039

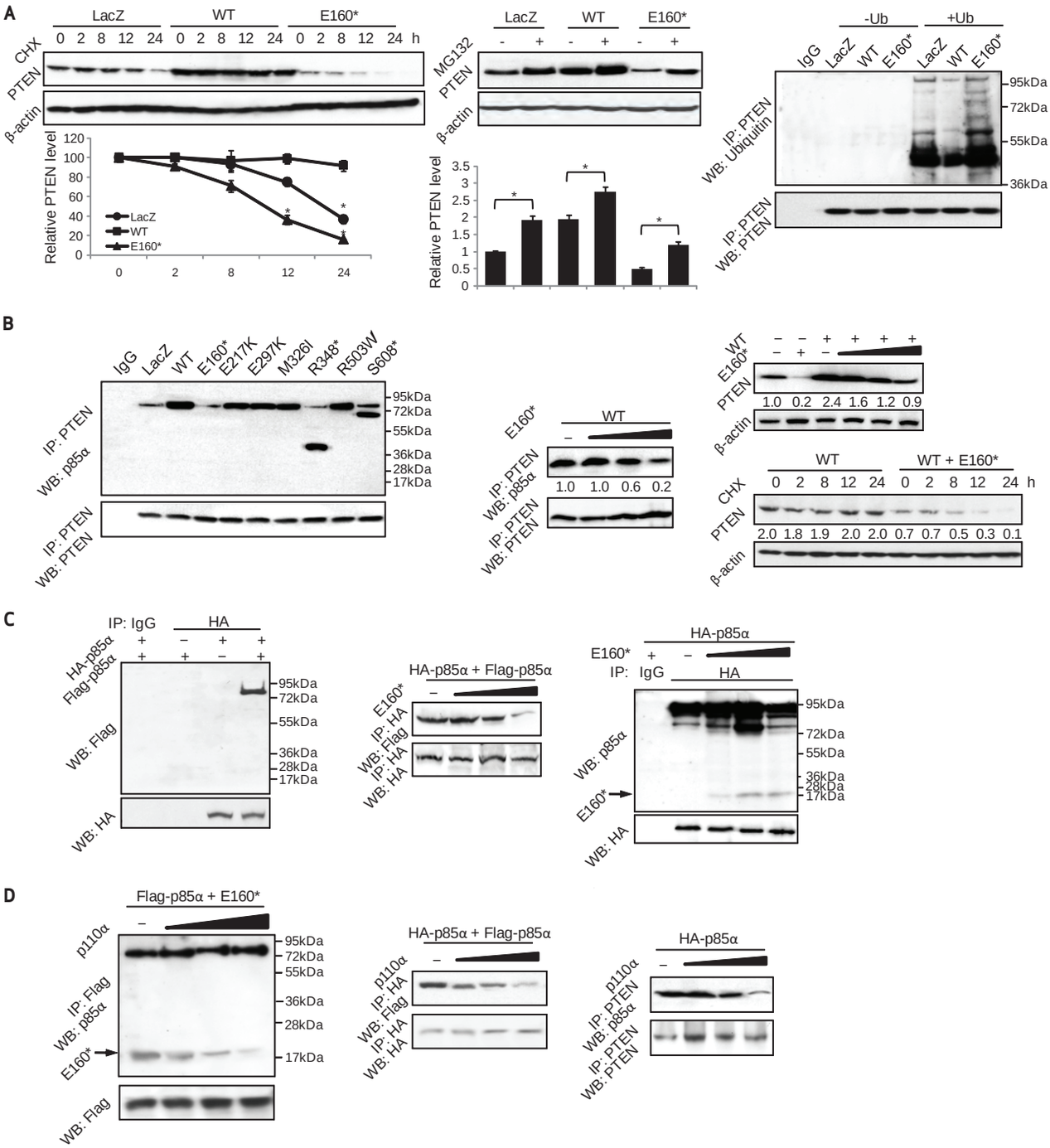

Figure 5. **A**, HEC1A cells transfected with LacZ or p85α WT or E160* were treated with cycloheximide (CHX; left) for indicated duration or with MG132 (center) for 24 hours. Cells were then harvested for WB. PTEN levels were normalized to β-actin by densitometry (below). *, $P < 0.05$. Right, HEC1A cells were transfected with LacZ or WT or E160* in the absence or presence of ubiquitin (Ub) for 72 hours. Whole-cell lysates were collected for IP with anti-PTEN and then subjected to WB with anti-ubiquitin. PTEN protein levels were normalized prior to IP by using proportionally different amounts of lysates. **B**, left, HEC1A cells were transfected with LacZ or WT or its mutants for 72 hours and were collected for IP with PTEN and WB with anti-p85α. HEC1A cells were co-transfected with WT or increasing amount of E160*. Cell lysates were collected for IP (center) or WB (right top). Right bottom, transfected HEC1A cells were treated with CHX for the indicated time points and harvested for WB. **C**, cells were transfected with HA-tagged p85α (*HA-p85α*) and/or Flag-tagged p85α (*Flag-p85α*) in the absence (left) or presence (center) of increasing amounts of E160*. IP was performed with anti-HA and WB with anti-Flag. Right, cells were transfected with HA-p85α and increasing amounts of E160*. IP was performed with anti-HA and WB with anti-p85α. **D**, left, cells were transfected with WT p110α, Flag-p85α, and E160*. IP was performed with anti-Flag and WB with anti-p85α. Center, cells were transfected with WT p110α, Flag-p85α, and HA-p85α. IP was performed with anti-HA and WB with anti-Flag. Right, cells were transfected with WT p110α and HA-p85α, IP was performed with PTEN and WB with p85α. Numerical values below each lane of the immunoblots represent quantification of the relative protein level by densitometry.

Published OnlineFirst June 7, 2011; DOI:10.1158/2159-8290.CD-11-0039

the endometrioid component is dominant at least in terms of mutational status. MMMT is poorly characterized to date. In addition to the frequent *TP53* mutations previously reported (28), we noted a low rate of aberrations in the PI3K pathway, *KRAS*, and *CTNNB1* in MMMT, clearly suggesting that MMMT has more in common mutationally with type 2 EC (serous and clear cell), in which *TP53* mutation is the most common genetic alteration and is considered an early event (29).

Based on frequent aberrations in *PIK3CA* and *PTEN*, we explored whether mutations in other members of the PI3K pathway are present in EC. Strikingly, the mutation rate of *PIK3R1* (20%) was markedly higher in EC than that previously reported for any other lineage, demonstrating selective targeting in EC (17, 18). In the COSMIC database (30), *PIK3R1* mutations were detected in 36 of 1693 (2%) tumors. *PIK3R2* mutation had only been reported in 1 of 108 (0.9%) colon cancers (18) and in 3 of 817 (0.4%) tumors (30). Our studies demonstrated *PIK3R2* mutations in 5% of EC, with several mutations being demonstrated to exhibit gain of function, establishing *PIK3R2* as a novel cancer gene.

Previous reports suggested that *KRAS* and *PIK3CA* mutations are mutually exclusive in EC (7, 14). However, these studies only sequenced exons 9 (helical) and 20 (catalytic domain) of *PIK3CA* in small sample sets. The large sample size in this study, the characterization of multiple PI3K pathway members, and our observation that *PIK3CA* mutations commonly occur outside of exons 9 and 20 likely accounts for the discrepancy, supporting our observation that *KRAS* and PI3K pathway members are coordinately mutated in EC. The concurrent mutations in PI3K pathway members and *KRAS* in cell lines support the concept that the mutations occur in a single cell population rather than in independent subclones. This may reflect, in part, a lack of functional redundancy among PI3K pathway and *KRAS* mutations in EC that is supported by RPPA demonstrating distinct downstream signaling consequences associated with these mutations. This activation of different pathways could thus cooperate for efficient transformation.

Co-mutations in different components of the PI3K pathway might also cooperate for efficient transformation (31). Further, we have demonstrated that PTEN protein loss and *PIK3CA* mutations have markedly different functional effects on PI3K pathway activation in human breast cancer (22). Co-mutations in PI3K pathway members in EC occur at frequencies significantly higher than predicted, in contrast to most cancers (19, 20). PTEN protein loss, regardless of *PTEN* mutational status, resulted in PI3K pathway activation. *PIK3CA, PIK3R1*, or *PIK3R2* mutation was more common in cells where PTEN protein was retained, and these mutations phenocopy the functional effects of PTEN loss on downstream signaling. MMR deficiency, which is an early event in the pathogenesis of EC (21), might contribute to these co-mutations. However, the mutations in the PI3K pathway members were not typical of MMR aberrations.

The majority of PTEN mutations in EC are heterozygous. PTEN haploinsufficiency has been reported to contribute to development of prostate cancer (32). However, despite PTEN mutations being heterozygous, almost half of EC demonstrated complete loss of PTEN protein, suggesting that additional mechanisms contribute to PTEN loss. Further, PTEN loss was also seen in a significant fraction of WT PTEN tumors. PTEN protein levels and function are extensively regulated by multiple genomic and epigenetic mechanisms in addition to mRNA and protein modification, emphasizing the importance of this tumor suppressor (25). Thus multiple mechanisms are likely to converge on regulation of PTEN protein levels and function in EC.

EC exhibits mutations throughout the coding region of *PIK3CA* with the exception of the RAS binding domain compatible with interactions with RAS being critical to the function of p110 (33). Consistent with a recent study, we observed a high frequency of mutations within the ABD domain in *PIK3CA*, compared to other tumor lineages (34). Interestingly, 87% of mutations within the ABD domain were associated with *PTEN* heterozygous mutation, suggesting that ABD mutations may selectively interact with *PTEN* heterozygous mutations. ABD domain mutations have been suggested to have lower transforming activity and to activate AKT to a lesser degree than catalytic and helical domain mutations (31, 34). It is possible that co-mutation of the ABD domain with *PTEN* increases information flow through the PI3K pathway. Although complete PTEN loss has been reported to elicit senescence in prostate cancer models (35), it does not appear to do so in EC, as several tumors did exhibit complete PTEN loss. Furthermore, although PTEN loss is often a late event in prostate tumorigenesis, PTEN aberrations occur early during the pathogenesis of EC.

The roles of p85 in PI3K pathway activation and tumorigenesis are complex. Levels of p85α are decreased in a number of tumor lineages (36). Haploinsufficiency of *PIK3R1* can result in PI3K pathway activation, whereas homozygous depletion inhibits the pathway (37). On the other hand, *PIK3R1* knockout mice demonstrated increased PI3K pathway activity and decreased PTEN protein levels, compatible with our data on the effect of WT p85α on PTEN levels (36). If in excess of p110, p85 could compete with the p85–p110 complex for binding to phosphorylated insulin receptor substrate (IRS) or to other phosphotyrosine-containing proteins, suggesting that free p85 could negatively modulate PI3K signaling (37). A direct and possibly bidirectional interaction between the N-terminal SH3-Rho-GAP domain of p85 and PTEN has been demonstrated (26, 38, 39). We showed herein that this p85α-PTEN interaction is associated with increased PTEN stability through decreased ubiquitination. The truncated gain-of-function mutant E160*, which does not bind either p110α or PTEN, binds WT p85α and decreases its binding to PTEN, resulting in PTEN destabilization through ubiquitination.

Overall, the data are most compatible with a model wherein free p85α forms a homodimer that is able to bind PTEN (Fig. 6). This model is supported by evidence that (1) overexpression of p85α did not increase p110α levels, indicating that p85α is not limiting in the cells; (2) p110α is not part of the complex because p110α overexpression inhibited p85α-PTEN interaction, suggesting a mutually exclusive binding; (3) E160* binds to free p85α because overexpression of p110α competed with E160* for binding to p85α; and (4) p85α self-dimerized and this homodimerization was inhibited by overexpression of p110α and E160*. The SH3

Published OnlineFirst June 7, 2011; DOI:10.1158/2159-8290.CD-11-0039

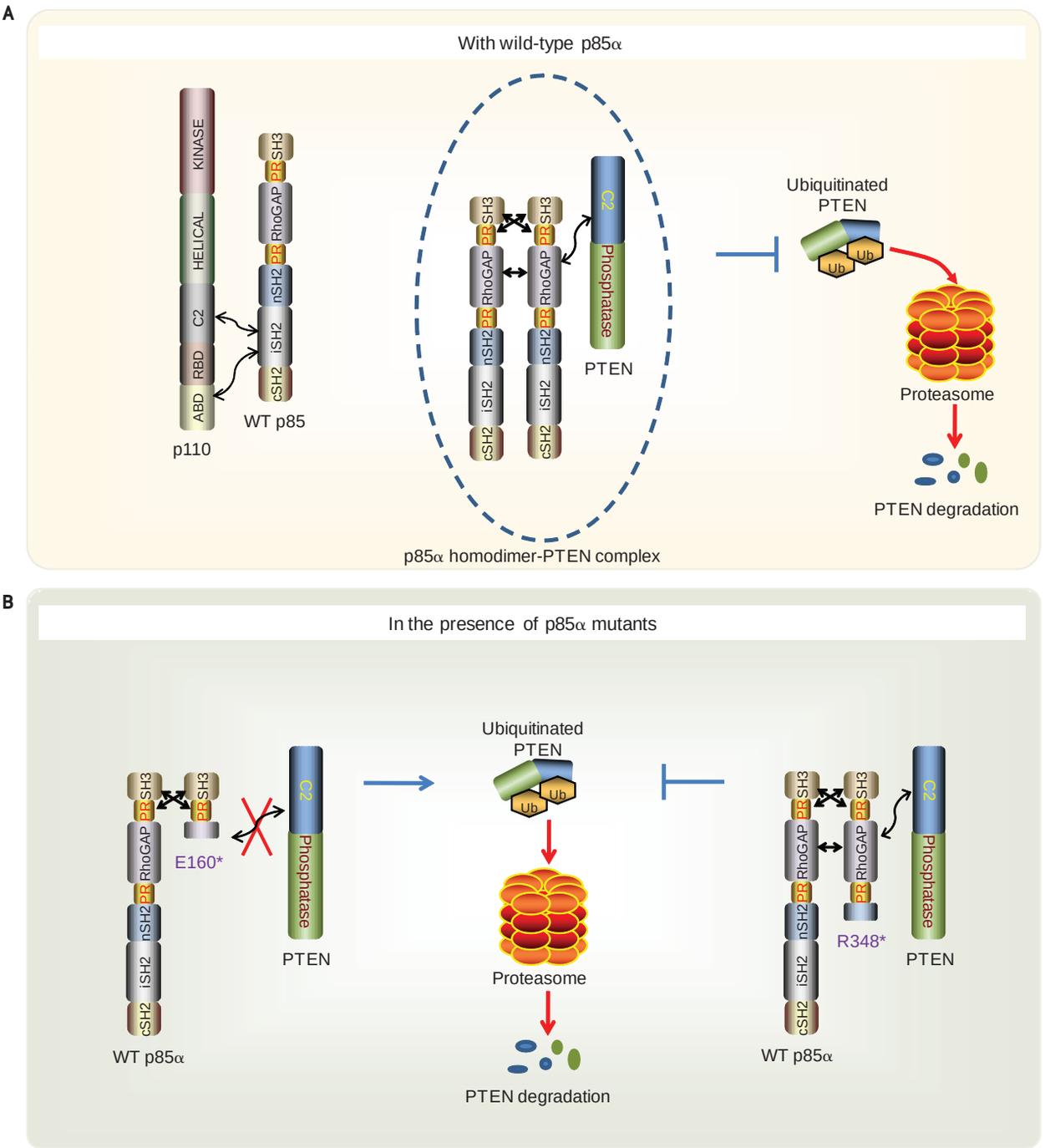

Figure 6. Schematic working model of p85α-mediated PTEN stabilization. **A**, in cells with WT p85α, in addition to p110α-bound p85α, excess p85α forms homodimers via intermolecular interactions between SH3 and proline-rich motif and between Rho-GAP domains (see Discussion). The homodimer likely undergoes conformation changes that allow binding to PTEN and stabilizes PTEN through inhibition of ubiquitination. **B**, the E160* truncated mutant binds WT p85α but inhibits PTEN binding, resulting in PTEN degradation. However, the R348* mutant retains the ability to bind PTEN after dimerization, either alone or with WT p85α, thereby inhibiting PTEN degradation. PR, proline-rich motif.

and first proline-rich motif have been shown to be sufficient to mediate homodimerization; furthermore, the truncated isoform p55γ, which lacks the N-terminal domains, failed to form dimers (27). Intermolecular interaction between Rho-GAP domains might also contribute to the p85α homodimer formation (27). The ability of E160* to bind with WT p85α suggests that SH3 and the first proline-rich domains constitute a major homodimerization interface. However, the failure of the E160*–p85α heterodimer to bind and stabilize PTEN whereas the R348*–p85α heterodimer

Published OnlineFirst June 7, 2011; DOI:10.1158/2159-8290.CD-11-0039

(or possibly R348* homodimers) binds and stabilizes PTEN, suggests that the Rho-GAP domain likely plays a role in the conformation change in p85α required for binding to PTEN. How the homodimer enhances PTEN stability warrants further investigation, but it is tempting to speculate that the homodimer may provide a combinatorial binding site for PTEN or may facilitate recruitment of other molecules to the complex to stabilize PTEN. Phosphorylation of the C-terminal tail of PTEN inhibits its proteosome-mediated degradation (40). p85 and unphosphorylated PTEN are part of a high molecular weight complex with formation of the complex associated with diminished AKT activation (38). In this scenario, it is possible that phosphorylated PTEN adopts a closed conformation that results in lower affinity for the complex (41). The association of PTEN with p85α is readily observed in EEC in the absence of growth factor addition, in contrast to previous studies (26). This can be potentially due to the frequent presence of other activating mutations in EEC (Fig. 1). In contrast to studies in other systems (38), we were unable to find evidence for a trimeric (or tetrameric) complex of PTEN, p85α, and p110α by cross-immunoprecipitation in EEC (not presented). Further, the ability of exogenous p110α to decrease p85α homodimers and p85α–PTEN heterodimers suggests that in EEC, the binding of PTEN and p110α to p85α may be mutually exclusive, with p85α monomers interacting with p110α and dimers with PTEN. The spontaneous E160* mutation from EEC will provide a powerful tool to elucidate the mechanisms underlying these processes.

Other activating p85α mutations found in EC likely elucidate additional regulatory mechanisms as they do not apparently alter PTEN protein levels but do increase pAKT levels. Three of five activating mutations identified in the Ba/F3 assay reside in the iSH2 domain, which binds the C2 domain of p110 inhibiting the catalytic activity of p110. These activating mutations appear to disrupt iSH2–C2 contact, releasing the inhibitory effect on p110 while retaining the ability to stabilize p110 (24, 42). One of the novel activating mutations in EC (R503W) is part of an exposed surface composed of basic residues that may bind to negatively charged membrane phosphatidylinositide substrates compatible with an independent mechanism (43).

The recurrent R348* activating mutation lacks intact SH2 and iSH2 domains and thus lacks ability to bind p110. It demonstrated lower activity than E160* in multiple repeat Ba/F3 assays. The portion of p85α remaining in the R348* mutant is similar to the minimal domain defined to bind PTEN (26), a property we confirmed for R348*, which may contribute to its activity. Because the R348* mutation is heterozygous in each of the 5 tumors, p110 might be stabilized by intact p85α expressed from the remaining *PIK3R1* allele. Indeed, an artificial p85α mutant unable to bind p110 has been demonstrated to increase kinase activity of a p110α mutant (44). Interestingly, heterozygous mutations in *PTEN* and/or *PIK3CA* were concurrent in tumors harboring the R348* mutation, suggesting that the activity of this mutant is most clearly manifest in cooperation with other mutants in the PI3K pathway.

Thus, there appear to be multiple mechanisms by which aberrations in *PIK3R1* can contribute to tumorigenesis. It is premature to predict the pathophysiologic relevance of the types of *PIK3R1* mutations on tumor initiation and progression. Possibly the different mutations will contribute to sensitivity to a specific type of PI3K pathway inhibitor. Therefore, the effects of each class of *PIK3R1* mutations on tumor initiation and progression warrant further study.

WT p85β demonstrated greater ability to induce Ba/F3 survival than WT p85α. Unlike p85α, p85β did not stabilize PTEN protein in spite of its ability to bind PTEN (unpublished data). It is possible that the two isoforms mediate different functions (45). Another plausible explanation is that the effects of p85α on PTEN are dominant over p85β when both isoforms are expressed. Indeed, we found that expression of exogenous p85α inhibited binding of p85β to PTEN (unpublished observation), suggesting that PTEN interacts preferentially with p85α. This finding is in contrast to previous studies in other cell lines where p85β appears to be the preferred partner of PTEN (39) and may represent the unique context of EEC cells. Of note, p85α and p85β share only 30% protein homology in the Rho-GAP domain that contributes to PTEN binding, in contrast to 80% in the SH2 domains. Although p85β possesses similar proline-rich motifs as p85α, whether p85β homodimerizes and/or bind PTEN as efficiently as p85α is unclear and may be context dependent. Therefore, due to the complex effects of p85α and p85β on the PI3K pathway, tumor development is likely to be tissue context dependent and determined by relative levels and activities of p110, p85, PTEN and phosphotyrosine residues.

Germline variants of *PIK3R1* (M326I) and *PIK3R2* (V727T) were found in our samples, with homozygous mutations occurring in frequencies fitting Hardy-Weinberg equilibrium. Although M326I has been reported to exhibit increased binding to IRS-1, it had no impact on PI3K activity and signaling events (46). Herein, we found that M326I and V727T had no effect on Ba/F3 survival or AKT phosphorylation. RPPA analysis also showed no difference in downstream signaling between patients with or without these variants (data not shown).

The prevalence of abnormalities in members of the PI3K pathway and *KRAS* implicates these pathways as critical drivers of pathogenesis of EC and thus as exciting targets for cancer treatment. Encouragingly, we found that mutations in the PI3K pathway and *KRAS* predict *in vitro* sensitivity to rapamycin and MEK inhibitor but, like other studies, not to GDC-0941 (47). Due to feedback loops in the PI3K pathway, rational targeted therapeutic combinations may be required for optimal outcomes. Our data also suggest that EEC cells with both PI3K pathway and *KRAS* mutations are relatively more resistant to PI3K pathway inhibitors than those with PI3K pathway aberrations alone, as previously observed (48, 49). Whether coordinate targeting of the PI3K and RAS pathways will demonstrate higher activity with acceptable toxicity in EC xenografts is under investigation. Further, we found that EC patients with PI3K pathway aberration appear to have a significantly lower recurrence risk ($P = 0.003$), suggesting that PI3K pathway mutation status might also predict tumor recurrence.

Currently, the choice of therapy for individual patients with EC is largely empirical. Our data, which include comprehensive characterization of genetic alterations coupled with mechanistic studies, suggest that manipulation of the PI3K

Published OnlineFirst June 7, 2011; DOI:10.1158/2159-8290.CD-11-0039

and RAS pathways could provide a promising molecular-targeted therapy in EC. The genomic and protein signatures we identified should affect the stratification of patients in trials and hence accelerate the fulfillment of personalized molecular medicine.

METHODS

Patient Samples

Endometrial tumor samples (26 EEC grade 1, 106 EEC grade 2, 29 EEC grade 3, 60 mixed endometrioid and serous, 18 MMMT, 4 serous) were obtained under institutional review board–approved protocols from 243 patients who were diagnosed at the MD Anderson Cancer Center (Houston, Texas) from 1998 to 2009. Specimens were reviewed by a pathologist (R.R. Broaddus) for ≥80% tumor content, histologic verification, and classification by grade and stage.

Cell Cultures and Plasmids

For descriptions of the cell lines used, see Supplementary Data. DNA fingerprinting (STR analysis) was performed for the characterization of cell lines.

Full-length open reading frames of *PIK3R1* and *PIK3R2* were cloned into pLenti-7.3 Dest lentiviral expression system (Invitrogen). Mutations were generated by site-directed mutagenesis using QuikChange II XL Site-Directed Mutagenesis Kit (Agilent Technologies). Four *PIK3R1* mutants were kindly provided by Dr. Lynda Chin (Harvard Medical School, Boston, Massachusetts). All constructs were confirmed by Sanger sequencing. Transfection was performed using Lipofectamine 2000 (Invitrogen).

Mutational Analysis

DNA preparation

Genomic DNA from frozen tumor resections or endometrial tumor cell lines was extracted using QIAamp DNA Mini Kit (Qiagen). Normal DNA was extracted from peripheral blood leukocytes using QIAamp Blood kit (Qiagen).

SNP analysis

A mass spectroscopy–based approach was used to detect SNPs (MassARRAY, Sequenom) as described previously (22). We designed high-throughput assays for somatic hotspot mutations in *KRAS, PIK3CA*, *CTNNB1*, *BRAF* and *AKT*. Mutations in the panel are listed in Supplementary Data.

Whole-gene resequencing

Resequencing of *PTEN*, *PIK3CA*, *PIK3R1*, *PIK3R2*, *FGFR2*, *TP53*, and *CTNNB1* was performed at the Human Genome Sequencing Center at the Baylor College of Medicine (Houston, Texas). The last exon of PTEN failed to amplify. All other sequencing covered all exons and intron–exon boundaries.

Ninety-two percent of *PIK3CA* mutations and 89% of *CTNNB1* mutations detected by Sanger sequencing were confirmed by MassARRAY (Sequenom), indicating a high accuracy of base-calling.

Mutations verification

PI3KR1 and *PIK3R2* mutations detected by resequencing were confirmed by independent PCR-based sequencing in the MD Anderson Cancer Center Sequencing Core. Variants were deemed somatic if they were absent in matched normal DNA.

Reverse-phase protein array

High-throughput RPPA for 127 proteins (antibody list provided in Supplementary Data) was performed as described previously (22, 50).

Ba/F3 cell viability assay

Lentiviruses carrying WT or mutated *PIK3R1* or *PIK3R2* were generated by cotransfection of HEK293FT cells with the constructs and ViralPower Lentiviral Expression System. Ba/F3 cells were incubated with the viral supernatant supplemented with IL-3. At 48 hours postinfection, the cells were washed three times with PBS and resuspended in medium without IL-3. Cells (2×10^4) were plated in 96-well plate and cultured for 4 weeks. CellTiter-Blue (Promega) was used to assess cell viability.

Statistical Analysis

To test the significance of pairwise comparisons between aberrations, we applied Tukey's Honestly Significant Difference (HSD) test to a 1-way ANOVA model. The analysis was performed with the R software (http://www.r-project.org/). Difference was considered significant when $P < 0.05$.

Additional experimental procedures are available in the Supplementary Data.

Disclosure of Potential Conflicts of Interest

G.B. Mills received commercial research grants from AstraZeneca, GlaxoSmithKline, Celgene, Exelixis, Roche, and Wyeth/Pfizer, and served as consultant to AstraZeneca, Celgene, Enzon, Novartis, and Wyeth/Pfizer. The other authors disclosed no potential conflicts of interest.

The Editor-in-Chief of *Cancer Discovery* is an author of this article. In keeping with the AACR's Editorial Policy, the paper was peer reviewed and a member of the AACR's Publications Committee rendered the decision concerning acceptability.

Acknowledgments

We thank Drs. Lynda Chin and Peter Vogt for providing p85α plasmids; and CCSG DNA analysis facility, RPPA core, and characterized cell line core (funded by NCI CA16672) in the MD Anderson Cancer Center. We wish to acknowledge the contributions of the Baylor College of Medicine Human Genome Sequencing Center and in particular, Dr. Richard Gibbs, director, Donna Muzny, Dr. David Wheeler, Lora Lewis, Robert Ruth, Kyle Chang, Humeira Akbar, and Shannon Gross.

Grant Support

This work was supported by a Stand Up to Cancer grant to L.C. Cantley, A.P. Myers, and G.B. Mills; a Uterine Cancer SPORE grant (NIH/NCI P50 CA098258) to R.R. Broaddus, K.H. Lu, and G.B. Mills; and a Career Development Award from the Conquer Cancer Foundation of the American Society of Clinical Oncology to B.T. Hennessy.

Received February 26, 2011; revised April 21, 2011; accepted May 12, 2011; published OnlineFirst June 7, 2011.

REFERENCES

1. Hennessy BT, Smith DL, Ram PT, Lu Y, Mills GB. Exploiting the PI3K/AKT pathway for cancer drug discovery. Nat Rev Drug Discov 2005;4:988–1004.
2. Daikoku T, Hirota Y, Tranguch S, Joshi AR, DeMayo FJ, Lydon JP, et al. Conditional loss of uterine Pten unfailingly and rapidly induces endometrial cancer in mice. Cancer Res 2008;68:5619–27.
3. Mutter GL, Ince TA, Baak JP, Kust GA, Zhou XP, Eng C. Molecular identification of latent precancers in histologically normal endometrium. Cancer Res 2001;61:4311–4.
4. Sun H, Enomoto T, Fujita M, Wada H, Yoshino K, Ozaki K, et al. Mutational analysis of the PTEN gene in endometrial carcinoma and hyperplasia. Am J Clin Pathol 2001;115:32–8.

Published OnlineFirst June 7, 2011; DOI:10.1158/2159-8290.CD-11-0039

5. Kanamori Y, Kigawa J, Itamochi H, Shimada M, Takahashi M, Kamazawa S, et al. Correlation between loss of PTEN expression and Akt phosphorylation in endometrial carcinoma. Clin Cancer Res 2001;7:892–5.
6. Quddus MR, Ologun BA, Sung CJ, Steinhoff MM, Lawrence WD. Utility of PTEN expression of endometrial "surface epithelial changes" and underlying atypical endometrial hyperplasia. Int J Gynecol Pathol 2009;28:471–6.
7. Velasco A, Bussaglia E, Pallares J, Dolcet X, Llobet D, Encinas M, et al. PIK3CA gene mutations in endometrial carcinoma: correlation with PTEN and K-RAS alterations. Hum Pathol 2006;37:1465–72.
8. Hayes MP, Douglas W, Ellenson LH. Molecular alterations of EGFR and PIK3CA in uterine serous carcinoma. Gynecol Oncol 2009;113:370–3.
9. Shoji K, Oda K, Nakagawa S, Hosokawa S, Nagae G, Uehara Y, et al. The oncogenic mutation in the pleckstrin homology domain of AKT1 in endometrial carcinomas. Br J Cancer 2009;101:145–8.
10. Dutt A, Salvesen HB, Chen TH, Ramos AH, Onofrio RC, Hatton C, et al. Drug-sensitive FGFR2 mutations in endometrial carcinoma. Proc Natl Acad Sci U S A 2008;105:8713–7.
11. Moreno-Bueno G, Hardisson D, Sanchez C, Sarrio D, Cassia R, Garcia-Rostan G, et al. Abnormalities of the APC/beta-catenin pathway in endometrial cancer. Oncogene 2002;21:7981–90.
12. Lax SF, Kendall B, Tashiro H, Slebos RJ, Hedrick L. The frequency of p53, K-ras mutations, and microsatellite instability differs in uterine endometrioid and serous carcinoma: evidence of distinct molecular genetic pathways. Cancer 2000;88:814–24.
13. Gupta S, Ramjaun AR, Haiko P, Wang Y, Warne PH, Nicke B, et al. Binding of ras to phosphoinositide 3-kinase p110alpha is required for ras-driven tumorigenesis in mice. Cell 2007;129:957–68.
14. Kang S, Seo SS, Chang HJ, Yoo CW, Park SY, Dong SM. Mutual exclusiveness between PIK3CA and KRAS mutations in endometrial carcinoma. Int J Gynecol Cancer 2008;18:1339–43.
15. Slomovitz BM, Lu KH, Johnston T, Coleman RL, Munsell M, Broaddus RR, et al. A phase 2 study of the oral mammalian target of rapamycin inhibitor, everolimus, in patients with recurrent endometrial carcinoma. Cancer 2010;116:5415–9.
16. Courtney KD, Corcoran RB, Engelman JA. The PI3K pathway as drug target in human cancer. J Clin Oncol 2010;28:1075–83.
17. Cancer Genome Atlas Research Network. Comprehensive genomic characterization defines human glioblastoma genes and core pathways. Nature 2008;455:1061–8.
18. Jaiswal BS, Janakiraman V, Kljavin NM, Chaudhuri S, Stern HM, Wang W, et al. Somatic mutations in p85alpha promote tumorigenesis through class IA PI3K activation. Cancer Cell 2009;16:463–74.
19. Broderick DK, Di C, Parrett TJ, Samuels YR, Cummins JM, McLendon RE, et al. Mutations of PIK3CA in anaplastic oligodendrogliomas, high-grade astrocytomas, and medulloblastomas. Cancer Res 2004;64:5048–50.
20. Murugan AK, Hong NT, Fukui Y, Munirajan AK, Tsuchida N. Oncogenic mutations of the PIK3CA gene in head and neck squamous cell carcinomas. Int J Oncol 2008;32:101–11.
21. Karamurzin Y, Rutgers JK. DNA mismatch repair deficiency in endometrial carcinoma. Int J Gynecol Pathol 2009;28:239–55.
22. Stemke-Hale K, Gonzalez-Angulo AM, Lluch A, Neve RM, Kuo WL, Davies M, et al. An integrative genomic and proteomic analysis of PIK3CA, PTEN, and AKT mutations in breast cancer. Cancer Res 2008;68:6084–91.
23. Samuels Y, Wang Z, Bardelli A, Silliman N, Ptak J, Szabo S, et al. High frequency of mutations of the PIK3CA gene in human cancers. Science 2004;304:554.
24. Sun M, Hillmann P, Hofmann BT, Hart JR, Vogt PK. Cancer-derived mutations in the regulatory subunit p85alpha of phosphoinositide 3-kinase function through the catalytic subunit p110alpha. Proc Natl Acad Sci U S A 2010;107:15547–52.
25. Salmena L, Carracedo A, Pandolfi PP. Tenets of PTEN tumor suppression. Cell 2008;133:403–14.
26. Chagpar RB, Links PH, Pastor MC, Furber LA, Hawrysh AD, Chamberlain MD, et al. Direct positive regulation of PTEN by the p85 subunit of phosphatidylinositol 3-kinase. Proc Natl Acad Sci U S A 2010;107:5471–6.
27. Harpur AG, Layton MJ, Das P, Bottomley MJ, Panayotou G, Driscoll PC, et al. Intermolecular interactions of the p85alpha regulatory subunit of phosphatidylinositol 3-kinase. J Biol Chem 1999;274:12323–32.
28. Taylor NP, Zighelboim I, Huettner PC, Powell MA, Gibb RK, Rader JS, et al. DNA mismatch repair and TP53 defects are early events in uterine carcinosarcoma tumorigenesis. Mod Pathol 2006;19:1333–8.
29. Jarboe EA, Pizer ES, Miron A, Monte N, Mutter GL, Crum CP. Evidence for a latent precursor (p53 signature) that may precede serous endometrial intraepithelial carcinoma. Mod Pathol 2009;22:345–50.
30. Forbes SA, Bindal N, Bamford S, Cole C, Kok CY, Beare D, et al. COSMIC: mining complete cancer genomes in the Catalogue of Somatic Mutations in Cancer. Nucleic Acids Res 2011;39: D945–50.
31. Oda K, Okada J, Timmerman L, Rodriguez-Viciana P, Stokoe D, Shoji K, et al. PIK3CA cooperates with other phosphatidylinositol 3′-kinase pathway mutations to effect oncogenic transformation. Cancer Res 2008;68:8127–36.
32. Kwabi-Addo B, Giri D, Schmidt K, Podsypanina K, Parsons R, Greenberg N, et al. Haploinsufficiency of the Pten tumor suppressor gene promotes prostate cancer progression. Proc Natl Acad Sci U S A 2001;98:11563–8.
33. Orme MH, Alrubaie S, Bradley GL, Walker CD, Leevers SJ. Input from Ras is required for maximal PI(3)K signalling in Drosophila. Nat Cell Biol 2006;8:1298–302.
34. Rudd ML, Price JC, Fogoros S, Godwin AK, Sgroi DC, Merino M, et al. A unique spectrum of somatic PIK3CA (p110a) mutations within primary endometrial carcinomas. Clin Cancer Res 2011;17:1331–40.
35. Alimonti A, Nardella C, Chen Z, Clohessy JG, Carracedo A, Trotman LC, et al. A novel type of cellular senescence that can be enhanced in mouse models and human tumor xenografts to suppress prostate tumorigenesis. J Clin Invest 2010;120:681–93.
36. Taniguchi CM, Winnay J, Kondo T, Bronson RT, Guimaraes AR, Aleman JO, et al. The phosphoinositide 3-kinase regulatory subunit p85alpha can exert tumor suppressor properties through negative regulation of growth factor signaling. Cancer Res 2010;70:5305–15.
37. Ueki K, Fruman DA, Brachmann SM, Tseng YH, Cantley LC, Kahn CR. Molecular balance between the regulatory and catalytic subunits of phosphoinositide 3-kinase regulates cell signaling and survival. Mol Cell Biol 2002;22:965–77.
38. Rabinovsky R, Pochanard P, McNear C, Brachmann SM, Duke-Cohan JS, Garraway LA, et al. p85 Associates with unphosphorylated PTEN and the PTEN-associated complex. Mol Cell Biol 2009;29:5377–88.
39. He J, de la Monte S, Wands JR. The p85beta regulatory subunit of PI3K serves as a substrate for PTEN protein phosphatase activity during insulin mediated signaling. Biochem Biophys Res Commun 2010;397:513–9.
40. Vazquez F, Ramaswamy S, Nakamura N, Sellers WR. Phosphorylation of the PTEN tail regulates protein stability and function. Mol Cell Biol 2000;20:5010–8.
41. Vazquez F, Grossman SR, Takahashi Y, Rokas MV, Nakamura N, Sellers WR. Phosphorylation of the PTEN tail acts as an inhibitory switch by preventing its recruitment into a protein complex. J Biol Chem 2001;276:48627–30.
42. Wu H, Shekar SC, Flinn RJ, El-Sibai M, Jaiswal BS, Sen KI, et al. Regulation of class IA PI 3-kinases: C2 domain-iSH2 domain contacts inhibit p85/p110alpha and are disrupted in oncogenic p85 mutants. Proc Natl Acad Sci U S A 2009;106:20258–63.
43. Huang CH, Mandelker D, Schmidt-Kittler O, Samuels Y, Velculescu VE, Kinzler KW, et al. The structure of a human p110alpha/p85alpha complex elucidates the effects of oncogenic PI3Kalpha mutations. Science 2007;318:1744–8.
44. Hsu JH, Shi Y, Frost P, Yan H, Hoang B, Sharma S, et al. Interleukin-6 activates phosphoinositol-3′ kinase in multiple myeloma tumor cells by signaling through RAS-dependent and, separately, through p85-dependent pathways. Oncogene 2004;23:3368–75.

Published OnlineFirst June 7, 2011; DOI:10.1158/2159-8290.CD-11-0039

45. Ueki K, Fruman DA, Yballe CM, Fasshauer M, Klein J, Asano T, et al. Positive and negative roles of p85 alpha and p85 beta regulatory subunits of phosphoinositide 3-kinase in insulin signaling. J Biol Chem 2003;278:48453–66.
46. Almind K, Delahaye L, Hansen T, Van Obberghen E, Pedersen O, Kahn CR. Characterization of the Met326Ile variant of phosphatidylinositol 3-kinase p85alpha. Proc Natl Acad Sci U S A 2002;99:2124–8.
47. O'Brien C, Wallin JJ, Sampath D, GuhaThakurta D, Savage H, Punnoose EA, et al. Predictive biomarkers of sensitivity to the phosphatidylinositol 3′ kinase inhibitor GDC-0941 in breast cancer preclinical models. Clin Cancer Res 2010;16:3670–83.
48. Ihle NT, Lemos R Jr Wipf P, Yacoub A, Mitchell C, Siwak D, et al. Mutations in the phosphatidylinositol-3-kinase pathway predict for antitumor activity of the inhibitor PX-866 whereas oncogenic Ras is a dominant predictor for resistance. Cancer Res 2009;69:143–50.
49. Engelman JA, Chen L, Tan X, Crosby K, Guimaraes AR, Upadhyay R, et al. Effective use of PI3K and MEK inhibitors to treat mutant Kras G12D and PIK3CA H1047R murine lung cancers. Nat Med 2008;14:1351–6.
50. Zhang L, Wei Q, Mao L, Liu W, Mills GB, Coombes K. Serial dilution curve: a new method for analysis of reverse phase protein array data. Bioinformatics 2009;25:650–4.